Two-dimensional Oscillation Program (TOP)

Daniel Roy Reese

LESIA, Paris Observatory

June 28, 2022

A brief history

LSB – Linear Solver Builder

- precursor to TOP
- perl interpreter to read equations
- Coriolis force, Lorentz force, centrifugal deformation
- **Main contributors:** Lorenzo Valdettaro, Michel Rieutord, François Lignières, Daniel R. Reese

A brief history

TOP – Two-dimension Oscillation Program

- 2007-2009: initial version
  - 1D and 2D real cases, then complex cases
  - adiabatic pulsations
- 2009-2011: extension to multi-domain calculations
- 2011-2013: inclusion of non-adiabatic effects
- 2014-2018:
  - various cases combined into 1 version of the code
  - inclusion of Python interface
  - development (still in progress) of a Domain Specific Language to simplify the coding of equations
- 2021: use of MAGMA library for GPU-based linear calculations
- 2022: quadruple precision version of TOP
- **Main contributors:** Daniel R. Reese, Bertrand Putigny, Alejandro Estaña, François Lignières, Michel Rieutord, Jérôme Ballot, Giovanni Mirouh

Overview

Two-dimensional Oscillation Program (TOP)

- code devised for calculating pulsations modes in rapidly rotating stellar models
- highly flexible approach which facilitates the inclusion of new physical ingredients

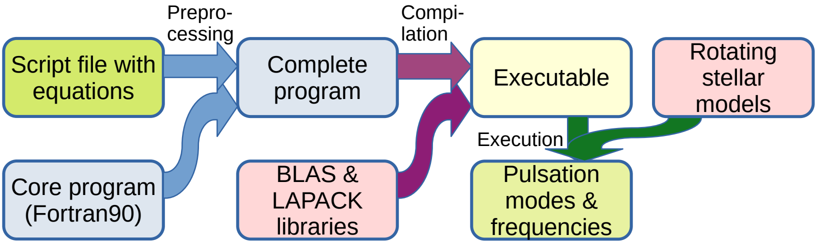

Equilibrium models

Polytropic models

- Lignières et al. (2006), Reese et al. (2006), Ballot et al. (2010)
- uniform rotation
- barotropic structure (lines of constant P, ρ coincide)

Equilibrium models

Polytropic models

- Lignières et al. (2006), Reese et al. (2006), Ballot et al. (2010)
- uniform rotation
- barotropic structure (lines of constant P, ρ coincide)

Self-Consistent Field (SCF) models

- Jackson et al. (2005), MacGregor et al. (2007)
- pre-imposed cylindrical rotation profile
- barotropic structure (lines of constant P, ρ, T coincide)
- energy equation applied on horizontal averages

Equilibrium models

Evolution STEllaire en Rotation (ESTER) models

- Espinosa Lara & Rieutord (2013), Rieutord et al. (2016)
- energy equation solved locally
- baroclinic structure (lines of constant P, ρ, T do not coincide)
- rotation profile deduced from baroclinic effects

Equilibrium models

Evolution STEllaire en Rotation (ESTER) models

- Espinosa Lara & Rieutord (2013), Rieutord et al. (2016)
- energy equation solved locally
- baroclinic structure (lines of constant P, ρ, T do not coincide)
- rotation profile deduced from baroclinic effects

Other models

- ASTEC models with perturbative deformation (Burke et al. 2011)
- CESAM models (ongoing work)
- preliminary calculations with ROTORC models (Deupree 1990, 1995)
- 1D Jupiter model subsequently deformed (Houdayer et al. 2019)

Pulsation equations

Continuity equation (conservation of mass)

$$0 = \frac{\delta \rho}{\rho_o} + \vec{\nabla} \cdot \vec{\xi}$$

Poisson's equation

$$0 = \Delta \Psi - 4 \pi G \left(\rho_o \frac{\delta \rho}{\rho_o} - \vec{\xi} \cdot \vec{\nabla} \rho_o \right)$$

$$\begin{aligned} \delta \rho &= \text{Lagrangian density perturbation} \\ \rho_o &= \text{equilibrium density profile} \\ \vec{\xi} &= \text{Lagrangian displacement} \\ \Psi &= \text{Eulerian perturbation to the gravitational potential} \end{aligned}$$

Pulsation equations

Euler's equations (conservation of momentum)

$$\begin{aligned}
0 &= [\omega + m\Omega]^2 \vec{\xi} - 2i\vec{\Omega} \times [\omega + m\Omega]\,\vec{\xi} - \vec{\Omega} \times \left(\vec{\Omega} \times \vec{\xi}\right) \\
&- \vec{\xi} \cdot \vec{\nabla}\left(\varpi \Omega^2 \vec{e}_\varpi\right) - \frac{P_o}{\rho_o}\vec{\nabla}\left(\frac{\delta P}{P_o}\right) + \frac{\vec{\nabla} P_o}{\rho_o}\left(\frac{\delta\rho}{\rho_o} - \frac{\delta P}{P_o}\right) - \vec{\nabla}\Psi \\
&+ \vec{\nabla}\left(\frac{\vec{\xi}\cdot\vec{\nabla}P_o}{\rho_o}\right) + \frac{\left(\vec{\xi}\cdot\vec{\nabla}P_o\right)\vec{\nabla}\rho_o - \left(\vec{\xi}\cdot\vec{\nabla}\rho_o\right)\vec{\nabla}P_o}{\rho_o^2}
\end{aligned}$$

$$\begin{aligned}
\omega &= \text{pulsation frequency} \\
m &= \text{azimuthal order} \\
\Omega &= \text{rotation profile} \\
\varpi &= \text{distance to the rotation axis} \\
\delta P &= \text{Lagrangian pressure perturbation}
\end{aligned}$$

Pulsation equations (adiabatic)

Adiabatic relation

$$\frac{\delta P}{P_o} = \Gamma_1 \frac{\delta \rho}{\rho_o}$$

- **advantages:** simplicity, provides accurate frequencies
- **disadvantages:**
  - no mode excitation
  - $\delta T_{\mathrm{eff}} / T_{\mathrm{eff}}$ not provided (approximated via $\delta T / T$)

Pulsation equations (non-adiabatic)

Energy conservation equation

- unperturbed form:

$$\rho_o T_o \frac{dS_o}{dt} = \epsilon_o \rho_o - \vec{\nabla} \cdot \vec{F}_o$$

- perturbed form:

$$\begin{aligned} i\left[\omega + m\Omega\right] \rho_o T_o \delta S &= \epsilon_o \rho_o \left(\frac{\delta\epsilon}{\epsilon_o} + \frac{\delta\rho}{\rho_o}\right) - \vec{\nabla} \cdot \delta\vec{F} \\ &+ \vec{\xi} \cdot \vec{\nabla}\left(\vec{\nabla} \cdot \vec{F}_o\right) - \vec{\nabla} \cdot \left[\left(\vec{\xi} \cdot \vec{\nabla}\right) \vec{F}_o\right] \end{aligned}$$

$\delta\vec{F}$ = Lagrangian perturbation to the energy flux

δS = Lagrangian entropy perturbation

$\delta\epsilon$ = Lagrangian perturbation to the energy production

Pulsation equations (non-adiabatic)

Energy flux

- total energy flux

$$\vec{F}_o = \vec{F}_o^{\mathrm{R}} + \vec{F}_o^{\mathrm{C}}$$

- unperturbed form of radiative energy flux:

$$\vec{F}_o^{\mathrm{R}} = -\frac{4acT_o^3}{3\kappa_o\rho_o}\vec{\nabla}T_o = -\chi_o\vec{\nabla}T_o$$

- perturbed form of radiative energy flux:

$$\begin{aligned} \delta\vec{F}^{\mathrm{R}} &= \left[(1+\chi_T)\frac{\delta T}{T_o} + \chi_\rho\frac{\delta\rho}{\rho_o}\right]\vec{F}_o^{\mathrm{R}} \\ &- \chi_o\left[T_o\vec{\nabla}\left(\frac{\delta T}{T_o}\right) + \vec{\xi}\cdot\vec{\nabla}\left(\vec{\nabla}T_o\right) - \vec{\nabla}\left(\vec{\xi}\cdot\vec{\nabla}T_o\right)\right] \end{aligned}$$

- frozen convection approximation:

$$\delta\vec{F}^{\mathrm{C}} \simeq \vec{0}$$

Pulsation equations (non-adiabatic)

Equation of state, opacities, and nuclear reaction rates

$$
\begin{aligned}
\frac{\delta P}{P_o} &= \Gamma_1 \frac{\delta\rho}{\rho_o} + P_{\mathrm{T}} \frac{\delta S}{c_{\mathrm{v}}} = P_\rho \frac{\delta\rho}{\rho_o} + P_{\mathrm{T}} \frac{\delta T}{T_o} \\
\frac{\delta T}{T_o} &= \frac{\delta S}{c_{\mathrm{v}}} + (\Gamma_3 - 1)\frac{\delta\rho}{\rho_o} = \frac{\delta S}{c_{\mathrm{p}}} + \nabla_{\mathrm{ad}} \frac{\delta P}{P_o} \\
\frac{\delta\chi}{\chi_o} &= \chi_\rho \frac{\delta\rho}{\rho_o} + \chi_T \frac{\delta T}{T_o} \\
\frac{\delta\epsilon}{\epsilon_o} &= \epsilon_T(\omega)\frac{\delta T}{T_o} + \epsilon_\rho(\omega)\frac{\delta\rho}{\rho_o}
\end{aligned}
$$

- in what follows we will neglect $\delta\epsilon$

Pulsation equations

Boundary conditions

- in the centre: regularity conditions
- at infinity: gravitational potential perturbation goes to zero
- at the surface:

$$\begin{aligned} \nabla_{\mathrm{vert.}} \left(\frac{\delta P}{P_o} \right) &= 0 \\ 4 \frac{\delta T}{T_o} &= \frac{\delta F^{\mathrm{R}}}{F_o^{\mathrm{R}}} \end{aligned}$$

Pulsation equations

Summary

- final result: a system of 10 equations with 10 unknowns:

$$\frac{\delta P}{P_o}, \quad \vec{\xi}, \quad \frac{\delta S}{c_\mathrm{p}}, \quad \delta \vec{F}^\mathrm{R}, \quad \frac{\delta T}{T_o}, \quad \Psi$$

- although some of these variables can be cancelled algebraically, they are needed to ensure good convergence

Numerical implementation

1. Express equations explicitly in spheroidal coordinates (ζ, θ, ϕ)

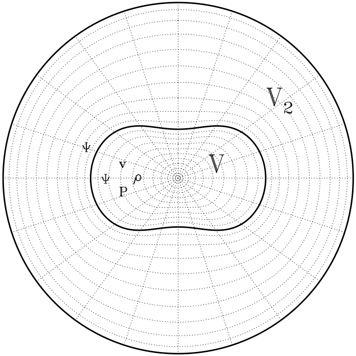

Numerical implementation

1. Express equations explicitly in spheroidal coordinates (ζ, θ, ϕ)

2. Express unknowns as a sum of spherical harmonics:

$$\Psi(r,\theta,\phi) = \sum_{\ell=|m|}^{\infty} \Psi_m^{\ell'}(\zeta) Y_{\ell'}^m(\theta,\phi)$$

Numerical implementation

1. Express equations explicitly in spheroidal coordinates (ζ, θ, ϕ)

2. Express unknowns as a sum of spherical harmonics:

$$\Psi(r,\theta,\phi) = \sum_{\ell=|m|}^{\infty} \Psi_m^{\ell'}(\zeta) Y_{\ell'}^m(\theta,\phi)$$

3. Project equations on spherical harmonic basis:

$$\iint_{4\pi} [\text{equation}] \left\{ Y_\ell^m \right\}^* \sin\theta \mathrm{d}\theta \mathrm{d}\phi$$

Horizontal discretisation – spectral approach

- rotation leads to couplings between the different spherical harmonics
  - the Coriolis force couples only adjacent harmonics (LSB more adapted to this situation)
  - the centrifugal deformation couples all harmonics

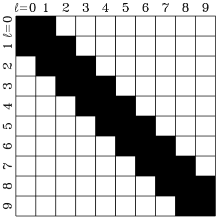

Coriolis force

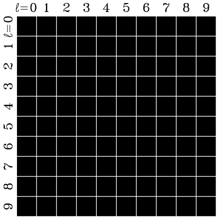

Centrifugal deformation

Horizontal discretisation – spectral approach

- symmetry with respect to the equator causes even and odd ℓ values to decouple
- allows us to increase the resolution
- toroidal component typically has the opposite parity

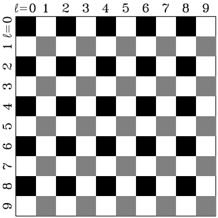

Numerical implementation

1. Express equations explicitly in spheroidal coordinates (ζ, θ, ϕ)
2. Express unknowns as a sum of spherical harmonics:

$$\Psi(r, \theta, \phi) = \sum_{\ell=|m|}^{\infty} \Psi_m^{\ell'}(\zeta) Y_{\ell'}^m(\theta, \phi)$$

3. Project equations on spherical harmonic basis:

$$\iint_{4\pi} [\text{equation}] \left\{ Y_\ell^m \right\}^* \sin\theta \mathrm{d}\theta \mathrm{d}\phi$$

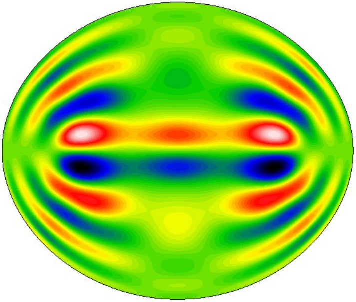

4. Discretise system in radial direction and solve:

$$\mathcal{A}\vec{x} = \omega \mathcal{B}\vec{x}$$

Solving the eigenvalue problem

Arnoldi-Chebyshev algorithm

- iterative approach for finding several eigenvalues and associated eigenfunctions with the largest amplitudes
- projects original matrix on smaller subspace with approximately equivalent solutions
  - search eigenvalues of smaller matrix with direct method

Solving the eigenvalue problem

Arnoldi-Chebyshev algorithm

- iterative approach for finding several eigenvalues and associated eigenfunctions with the largest amplitudes
- projects original matrix on smaller subspace with approximately equivalent solutions
  - search eigenvalues of smaller matrix with direct method

Spectral transformation

$$Av = \lambda Bv \;\Leftrightarrow\; (A - \sigma B)^{-1} Bv = \mu v \qquad \text{where} \qquad \lambda = \sigma + \frac{1}{\mu}$$

- when applying the Arnoldi-Chebyshev algorithm, or other iterative methods, we need to solve $(A - \sigma B)\, X = Y$
- it is therefore necessary to construct and factorise $A - \sigma B$

Polynomial eigenvalue problem

$$\sum_{i=0}^{n} \lambda^i A_i v = 0 \qquad \Longleftrightarrow \qquad \mathcal{A}x = \lambda \mathcal{B}x \qquad \text{where}$$

$$\mathcal{A} = \begin{bmatrix} A_0 & \cdot & \cdot & \cdot \\ \cdot & I_{\mathrm{d}} & \cdot & \cdot \\ & & \ddots & \\ \cdot & \cdot & & \cdot \\ \cdot & \cdot & \cdot & I_{\mathrm{d}} \end{bmatrix}, \quad \mathcal{B} = \begin{bmatrix} -A_1 & -A_2 & \cdots & -A_n \\ I_{\mathrm{d}} & \cdot & \cdot & \cdot \\ & \ddots & & \\ \cdot & & \cdot & \cdot \\ \cdot & \cdot & I_{\mathrm{d}} & \cdot \end{bmatrix}, \quad x = \begin{bmatrix} v \\ \lambda v \\ \vdots \\ \lambda^{n-1} v \end{bmatrix}$$

Solving $(\mathcal{A} - \sigma\mathcal{B})\, X = Y$

1. $X = [x_0 \ldots x_{n-1}]^T, \qquad Y = [y_0 \ldots y_{n-1}]^T$
2. By induction, let us define $(w_i)_{i \in [1, n-1]}$:
   $w_1 = \sigma y_1, \qquad w_{i+1} = \sigma(y_{i+1} + w_i)$
3. Solve: $x_0 = \left(\sum_{i=0}^{n} \sigma^i A_i\right)^{-1} \left(y_0 - \sum_{i=1}^{n-1} A_{i+1} w_i\right)$
4. By induction: $x_{i+1} = y_{i+1} + \sigma x_i$

Vertical discretisation – spectral approach

Characteristics

- exponential convergence rate
- fixed grid
- factorisation of full matrix
    - good parallelisation
- suitable for polytropic models

Illustration

- **Model**: polytrope
- **Resolution**: 5670×5670
    - $\mathrm{N}_r = 81$
    - $\mathrm{N}_t = 10$
- **Fill factor**: $10.6\,\%$

Matrix

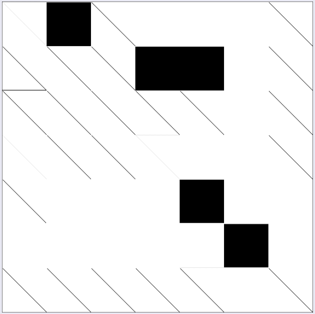

Vertical discretisation – finite-differences

Characteristics

- polynomial convergence
- flexible choice of grid
- factorisation of band matrix
  - poor parallelisation
- suitable for SCF models, Jupiter models

Illustration

- **Model**: SCF
- **Resolution**: 8080×8080
  - $(\mathrm{N}_r, \mathrm{N}_t) = (101, 10)$
  - Lower bands: 130
  - Upper bands: 140
- **Fill factor (in band)**: $27.0\,\%$

Matrix

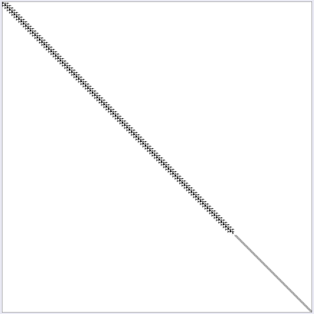

Vertical discretisation – spectral multi-domain

Characteristics

- exponential convergence
- flexible choice of domains
- factorisation of block tridiagonal matrix
  - good parallelisation
- suitable for ESTER models

Illustration

- **Model**: ESTER
- **Resolution**: 10150×10150
  - $\mathrm{N}_r = (30, 55, 45, 40, 40, 50, 70, 70, 30)$
  - $\mathrm{N}_t = 5$
- **Fill factor (tridiagonal blocs)**: 25.4 %

Matrix

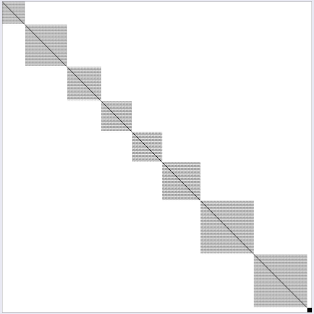

The multi-domain approach

- **assumption**: only consecutive domains are coupled
  $\Rightarrow$ tridiagonal block matrix

$$\begin{bmatrix} A_{11} & A_{12} & & \\ A_{21} & A_{22} & A_{23} & \\ & & \ddots & A_{n-1,\,n} \\ & & A_{n,\,n-1} & A_{n,\,n} \end{bmatrix} \begin{bmatrix} X_1 \\ X_2 \\ \vdots \\ X_n \end{bmatrix} = \begin{bmatrix} Y_1 \\ Y_2 \\ \vdots \\ Y_n \end{bmatrix}$$

Solving this system

- use of Gauss' pivot to eliminate $A_{i+1,\,i}$ and $A_{i,\,i+1}$
- one should not forget that matrix multiplication is not commutative

"Factorisation"

$$\tilde{A}_{11} = A_{11} \qquad \tilde{A}_{i+1,\,i+1} = A_{i+1,\,i+1} - A_{i+1,\,i}\tilde{A}_{i,\,i}^{-1}A_{i,\,i+1}$$

Downward sweep

$$\tilde{Y}_1 = Y_1 \qquad \tilde{Y}_{i+1} = Y_{i+1} - A_{i+1,\,i}\tilde{A}_{i,\,i}^{-1}\tilde{Y}_i$$

Upward sweep

$$X_n = \tilde{A}_{n,\,n}^{-1}\tilde{Y}_n \qquad X_{i-1} = \tilde{A}_{i-1,\,i-1}^{-1}\left(\tilde{Y}_{i-1} - A_{i-1,\,i}\tilde{X}_i\right)$$

Numerical cost for adiabatic calculations

N_r	N_h	Memory (in Gb)	Time (in min)	Num. proc.
400	10	0.5	0.16	2
400	15	1.1	0.33	2
400	20	1.9	0.65	2
400	30	4.2	1.6	2
400	40	7.4	3.3	2
400	100	$\sim$70	24	25

Numerical cost for non-adiabatic calculations

N_r	N_h	Memory (in Gb)	Time (in min)	Num. proc.
400	10	3.5		
400	15	7.9		
400	20	13.4	5	4
400	29	28.0	10	8
400	40	52.7	22	8
400	50	82.3	26	16

Estimated accuracy

Polytrope

- Variational principle: $\Delta\omega/\omega \sim 10^{-7}$ when $N = 3$ and $\Delta\omega/\omega \sim 10^{-5}$ when $N = 1.5$
- Numerically: $\Delta\omega/\omega \gtrsim 10^{-10}$
- Comparison with ACOR: $\Delta\omega/\omega \sim 10^{-6}$ to 5×10^{-3} (Ouazzani et al. 2012)

SCF

- Variational principle: $\Delta\omega/\omega \sim 10^{-3}$ to 10^{-2}
- Numerically: $\Delta\omega/\omega \sim 10^{-5}$ to 10^{-4}

Estimated accuracy

ESTER: adiabatic case

- Variational principle (continuous model): $\Delta\omega/\omega \sim 10^{-12}$ to 10^{-8}
- Variational principle (discontinous model): $\Delta\omega/\omega \sim 10^{-8}$ to 10^{-4}

ESTER: non-adiabatic case

- the problem is stiff: reduced numerical accuracy
- estimated accuracy based on variational expression:
  - frequencies: $\sim 10^{-4}$
  - excitation/damping rates: 10^{-2} to 10^{-1}
- stability may be improved through a hybrid approach: adiabatic in the centre, non-adiabatic near the surface

Mode classification

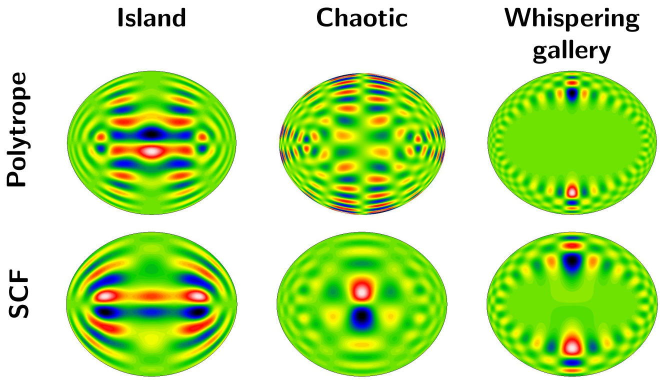

- classification of acoustic modes in polytropic models based on ray dynamics (Lignières & Georgeot, 2008, 2009)
- extended to realistic (SCF) models (Reese et al. 2009)
- automatic mode classification, tested on ESTER models (Mirouh et al. 2019)

Mode classification

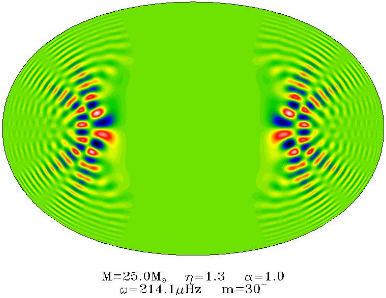

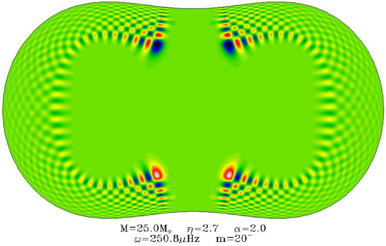

- some classes of modes persist even in highly distorted models

Discovery of rosette modes

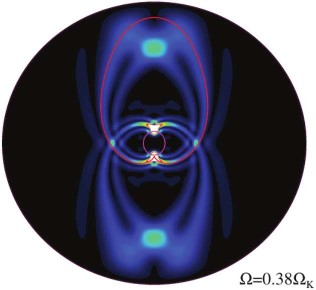

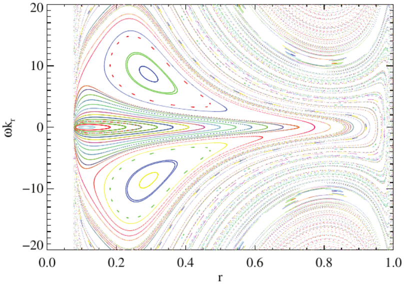

- discovery of Rosette modes (Ballot et al. 2012)

Non-adiabatic pulsations in ESTER models

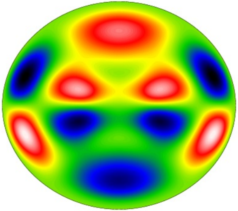

Acoustic

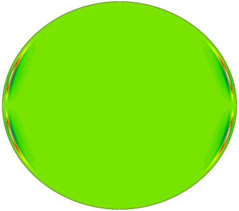

Work

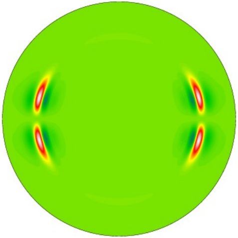

Work (vs. log T)

- red = driving regions
- blue = damping regions
- see Reese et al. 2017

Characterisation of rapidly rotating stars

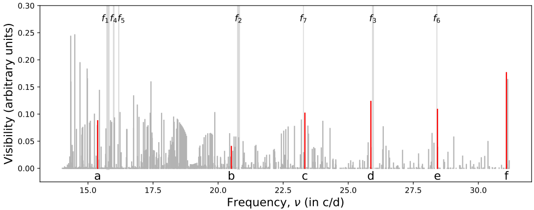

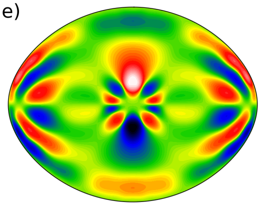

$\nu = 6.873$ c/d
$m = 0$, odd

- characterisation of Altair using interferometry, spectroscopy, and seismology (Bouchaud et al. 2020)
- characterisation of β Pic using multicolour photometry (Zwintz et al. 2019)

Conclusion

- TOP has played an important role in understanding pulsation modes in rapidly rotating stars
- it is starting to help us characterise such stars
- ongoing developments which should make TOP easier to use, thus facilitating new discoveries